Kunii, D., and O. Levenspiel "Fluidization Engineering," Wiley (1969).
Kunii, D., K. Yoshida, and O. Levenspiel, "Axial Movement of Solids in Bubbling Fluidized Solids Beds," *I. Chem. E. Symp. Ser.*, no. 30, p. 79 (1968).
Lewis, W. K., E. R. Gilliland, and H. Girouard, "Heat Transfer and Solids Mixing in Beds of Fluidized Solids," *Chem. Eng. Prog. Symp. Ser.*, no. 38 **58**, p. 87 (1962).
Makhorin, K. E., V. S. Pikashov, and G. P. Kuchin, "Measuring Particle Temperature and Emissivity in a High Temperature Fluidized Bed," *Fluidization*, Proceedings of the 2nd Eng. Fond. Conf., Cambridge University Press, p. 93 (1978).
Melamed, N. T., "Optical Properties of Powders: Part I. Optical Absorption," *J. of Applied Physics*, **34**, No. 3, p. 560 (1963).
Olalde, G., J. L. Peube, and M. Daguenet, "Theoretical Study of Gas Heated in a Porous Material Subjected to a Concentrated Solar Radiation," *Revue de Physique Appliquée*, **15**, p. 423 (1980).
Siegel, R., and J. R. Howel, "Thermal Radiation Heat Transfer," McGraw Hill (1972).
Ter Vrugt, "Optical Properties of Thin Powder Layers," Philips Res. Repts., **20**, p. 23 (1965).
Touloukian, Y. S., and O. P. De Witt, "Thermophysical Properties of Matter," 8, Ed. IFI Plenum (1972).
Wen, C. Y., and Y. H. Yu, "A Generalized Method for Predicting the Minimum Fluidization Velocity," *AIChE J.*, **12**, p. 610 (1966).

Manuscript received October 15, 1980; revision received August 5, and accepted August 24, 1981

Influence of Vapor Entrainment on Distillation Tray Efficiency at High Pressures

P. J. HOEK and F. J. ZUIDERWEG

Laboratory for Process Equipment
Delft University of Technology
Delft, The Netherlands

A recent publication of Fractionation Research Inc. (FRI) (Sakata and Yanagi, 1979) provides experimental evidence that tray efficiency initially rises with increasing pressure, reaches a maximum value, and then decreases again at very high pressures. It is shown in this paper that at these high pressures, significant amounts of vapor can be entrained with the downflowing liquid, e.g., abt. 50 mol per 100 mol liquid at 2,760 kPa. A new model is developed to determine the effect of vapor entrainment on tray efficiency. It is shown that the experimentally observed loss of tray efficiency corresponds with the entrainment rates found at high pressures.

SCOPE

At the Third International Symposium on Distillation in London, Sakata and Yanagi (1979) have reported on pressure drop, capacity, entrainment, weeping and tray efficiency of a commercial size 1.2-m diameter sieve tray. The experiments were carried out with two hydrocarbon systems over a wide range of pressures. This set of FRI data will probably prove to be quite useful for checking existing and developing new tray performance models. During the discussion at the symposium, Porter and Jenkins (1979) pointed out the relevance of the spray regime with regard to the FRI entrainment data.

It is the scope of the present study to offer an explanation for a remarkable trend in the FRI efficiency data; i.e., with increasing pressure, overall tray efficiency first increases but decreases again when the pressure rises over 1,140 kPa (Table 1).

Parallel with the efficiency loss at high pressures the capacity of the sieve tray is also strongly reduced. This can be seen from Figure 1 in which in the usual manner the "capacity factor" is plotted against the "flow parameter."

The loss of tray efficiency at high pressures is surprising, since with increasing pressure most of the physical properties of boiling homogeneous systems become continuously more favorable for enhancing mass transfer. In particular, the interfacial area will become very large because of the rapidly decreasing surface tension which reaches zero value at the critical pressure. Thus, the local point efficiency can be speculated to go up to 100% when the critical point is approached. It is, therefore, important first to analyze the suggested anomaly in the FRI high-pressure efficiency data before these data are used for the development of new tray efficiency correlations.

Sakata and Yanagi mention that at the very high pressures the capacity of the trays is limited by downcomer flooding; i.e., at the onset of flooding, the bed levels are still very low and practically no liquid is entrained with the vapor. This suggests that the downcomers are filled with foam; it is, therefore, conceivable that vapor is entrained with the liquid downflow to the next lower tray. In a recent paper, Lockett and Gharani (1979) confirm that at high downcomer velocities considerable amounts of vapor are entrained. However, they do not expect this entrainment to have a noticeable influence on tray efficiency at high pressures.

In the present study estimates are made on the average vapor content in the downcomer two-phase mixture by calculating the liquid backup at flooding. The resulting vapor entrainment is found by using Lockett and Gharani's (1979) ratio between the downcomer average vapor content and the vapor content of the downcomer underflow. In order to see if the quantities of entrained vapor thus found correspond with the observed efficiency losses, a new vapor entrainment/efficiency model is developed.

CONCLUSIONS AND SIGNIFICANCE

From the calculation of the vapor content in the downcomer two-phase mixture at flooding, it is concluded that at the highest FRI experimental pressures considerable amounts of vapor are entrained with the liquid downflow, e.g., at 2,760 kPa, about 50 kmol vapor per 100 kmol liquid. Further, the calculated entrainment rates correspond with the observed loss in overall tray efficiency under the condition that in the numerical evaluation

of the new entrainment/efficiency model the following assumptions hold:

a) The liquid flows over the plate in plugflow.

b) The "true" point efficiency at very high pressures can be obtained from point efficiencies at lower pressures by extrapolation against reduced pressure, taking a value of 100% at the critical point.

c) In the mass transfer process, liquid-side driving force is at high pressures more relevant than the same in terms of vapor-side driving force.

Notwithstanding the rather speculative methods employed in the analysis, it can be stated that the FRI data provide perhaps the first published evidence of vapor entrainment causing a noticeable decrease of tray efficiency. At the same time it is concluded that the FRI data as such can not be used for the development of new mass transfer correlations for trays. It is suggested to employ for this purpose the so-called "true" point efficiencies, obtained from the extrapolation against reduced pressure.

An additional interesting conclusion from the work on the entrainment-efficiency model is that vapor entrainment is not always detrimental to tray efficiency. At low point efficiencies and with liquid plug flow, vapor entrainment can cause a marked improvement of the overall efficiency.

THE PROBLEM

Distillation systems in which the pressure is continuously increased have the unique property that ultimately the difference in physical properties between vapor and liquid disappear. As a result, equipment performance can be expected to approach limiting values at the critical condition. As an example, the identity of vapor and liquid density will cause zero capacity at the critical point. This is confirmed by the FRI capacity data for total reflux distillation. Under such conditions, the flowparameter

$$FP = \frac{u_l}{u_g} \cdot \left(\frac{\rho_l}{\rho_g}\right)^{1/2} \tag{1}$$

is identical with the square root of the rates of vapor and liquid density:

$$FP_{(TR)} = \left(\frac{\rho_g}{\rho_l}\right)^{1/2} \tag{2}$$

Thus, at total reflux, the critical condition is identical with $FP = 1$. Figure 1 shows that in a plot of capacity factor (CF) against flow parameter, the total reflux data in point of fact extrapolate to CF = zero at $FP = 1$.

The approach of the critical condition also provides a boundary value for the mass transfer performance. The disappearing difference between vapor and liquid density and the approach to zero interfacial tension causes ideal mass transfer conditions, despite the decreasing vapor diffusivity. The case becomes identical with that of mixing two fluids which have the same physical properties. This implies that the point efficiency ($E_{p\text{-}og}$) extrapolates to 100%. In the FRI publication, the efficiencies are reported in terms of overall efficiency (E_o) instead of point efficiency. It can, nevertheless, be concluded that the trend in the data is quite contradictory with the expected improving mass transfer performance close to the critical point (Table 1).

It can be attempted to derive point efficiency from the overall efficiency data by using tray efficiency/flow models. Two models are of particular interest, i.e., the partial mixing model (e.g., Gerster et al., 1958) and the maldistribution model (Porter et al., 1972). For the case under consideration, the latter is of limited relevance, however, since the ratio of weir length to column diameter is close to unity ($W/D = 0.78$); further, the second controlling parameter, $\lambda E_{p\text{-}og}$ is relatively small, i.e., in the range 0.5 to 1.0. For the application of the partial mixing model, Peclet numbers have to be known. For this purpose, we developed a new correlation for sieve trays, based on the data of Barker and Self (1962), Porter et al. (1977), and additional data determined in our laboratory by Schoorl and Hofhuis. (Pe-numbers were determined in the same equipment as described by Hofhuis (1980) by use of the "back mixing" method. Liquid rates were resp. 1.5, 4 and 6.5 m^3 per hour per meter weir length.) This correlation is shown in Figure 2. For calculation of the Peclet number, the holdup h_l has to be obtained by the Hofhuis (1980) equation:

$$h_l = 0.6\, H_W{}^{1/2} P^{1/4} (25L\ H_W < 00\ \text{mm}) \left(\frac{FP}{b}\right)^{1/4} \tag{3}$$

The derived Peclet numbers for the FRI conditions are given in Table 2; they indicate that for all practical purposes, the flow over the plate can be identified as approximate plugflow. Therefore, the point efficiencies were calculated by the Lewis equation:

$$E_{m\text{-}og} = \frac{1}{\lambda}[\exp(\lambda\, E_{p\text{-}og}) - 1] \tag{4}$$

with

$$E_o = \frac{\log[1 + E_{m\text{-}og}(\lambda - 1)]}{\log\lambda} \tag{5}$$

The derived point efficiencies are also given in Table 2; they have been plotted in Figure 3 against reduced pressure. It is concluded that the trend of $E_{p\text{-}og}$ with pressure deviates fundamentally from the expected trend for which $E_{p\text{-}eg} = 100\%$ at $P_R = 1$.

TABLE 1. OVERALL EFFICIENCIES

Pressure, kPa	System	Range of E_o
28	C_6/C_7	70–80
165	C_6/C_7	90–95
1,140	C_4	120–125
2,070	C_4	105–110
2,760	C_4	95–100

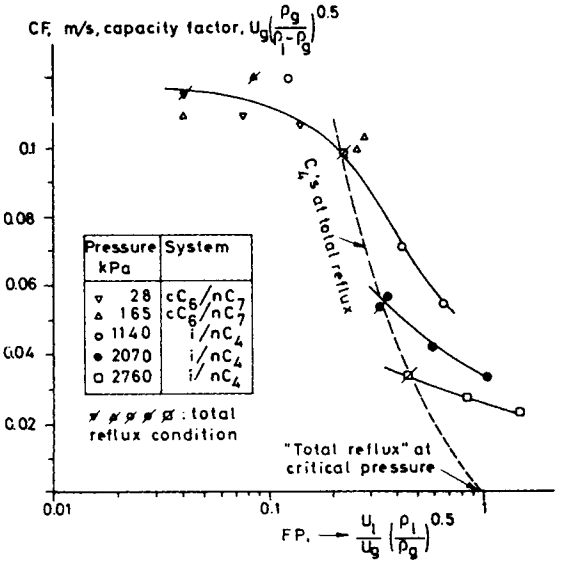

Figure 1. Capacity plot FRI sieve tray.

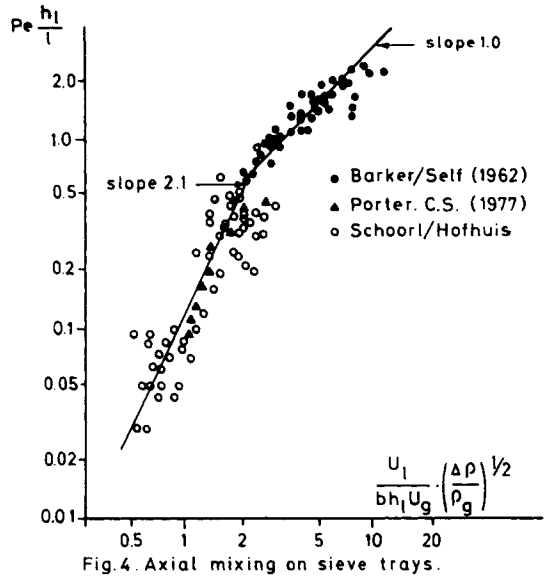

Fig.4. Axial mixing on sieve trays.

Figure 2. Correlation of Peclet numbers.

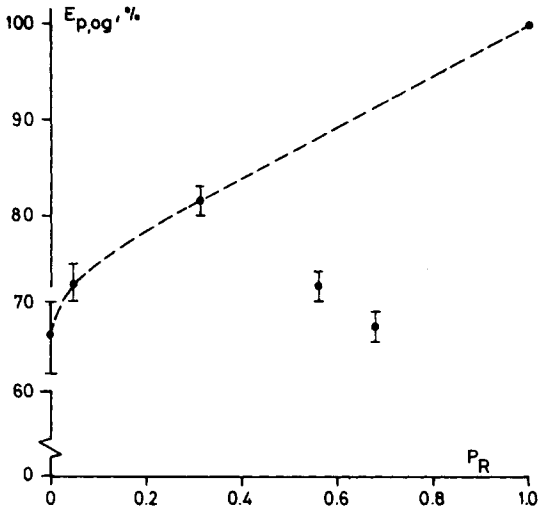

Figure 3. Plot of point efficiency against reduced pressure.

ESTIMATION OF VAPOR ENTRAINMENT

Recently, Lockett and Gharani (1979) reported on the entrainment of vapor with the downcomer liquid underflow. Defining with $\epsilon_{g,s}$ the vapor fraction in this underflow and with $\bar{\epsilon}_{g,d}$ the average fraction of vapor in the downcomer two-phase mixture, Lockett and Gharani's results can be generalized by plotting $\epsilon_{g,s}/\bar{\epsilon}_{g,d}$ as function of the two-phase downflow mixture velocity (Figure 4). The segregation of vapor and liquid in the downcomer, Figure 4, holds probably only for the test system applied, i.e., air-water. Since with low surface tension hydrocarbon vapor-liquid mixtures, the segregation will be less efficient it can be assumed that the curve in Figure 4 provides the minimum fraction of vapor in the downcomer underflow. The maximum is evidently obtained when no segregation occurs at all, i.e., $\epsilon_{g,s} = \bar{\epsilon}_{g,d}$.

From the above, it follows that a range of $\epsilon_{g,s}$ could be identified when $\bar{\epsilon}_{g,d}$ is known. The FRI paper provides no direct information on $\bar{\epsilon}_{g,d}$. However, reasonable estimates can be made for the point of incipient flooding. At this condition, the downcomer is just filled with two-phase mixture up to the weir. With ΔH = liquid backup in the downcomer it follows for $\bar{\epsilon}_{g,d}$

$$\bar{\epsilon}_{g,d} = \frac{H_T + H_W - \Delta H}{H_T + H_W} \tag{6}$$

The liquid backup ΔH can be calculated by

$$\Delta H = h_l + \frac{\Delta P}{g\Delta\rho} + \frac{(1-\beta^4)\,u_m^2\,\rho_m}{2C_D^2\,g\,\Delta\rho} \tag{7}$$

in which the underflow mixture velocity u_m is given by:

$$u_m = u_{l,s}/(1-\epsilon_{g,s}) \tag{8}$$

and the mixture density, ρ_m, by

$$\rho_m = (1-\epsilon_{g,s})\rho_l + \epsilon_{g,s}\rho_g \tag{9}$$

For the discharge coefficient an average value is proposed C_D = 0.8 (data of Hofhuis, 1980).

TABLE 2. PECLET NUMBERS AND POINT EFFICIENCIES

Pressure, kPa	P_R	Pe	Range of $E_{p\text{-}og}$, %
28	0.0075	8	63–71
165	0.045	18	71–75
1,140	0.31	33	80–83
2,070	0.56	42	71–74
2,760	0.68	44	67–70

The liquid velocity, pressure drop and holdup in the above equation are obtained from the points of incipient flooding. The latter may be determined when it is assumed that with increasing the tray loading beyond incipient flooding, the intertray spacing is rapidly filled up with two-phase mixture. This causes a sudden increase in tray pressure drop. To identify these points, we calculated the pressure drop curves and compared these with the experimental pressure drops. For the calculations we used the relation:

$$\Delta P = g\,h_l\rho_l + \frac{1}{2}\frac{\rho_g\,U_{g,h}^2}{C_D{}^2} \tag{10}$$

with C_D = 0.67. For h_l the Hofhuis equation (Eq. 3) was used.

The agreement between calculated and experimental pressure drop in the main operating range appears to be quite satisfactory as can be seen from Figure 5. Also, the points at which the pressure drop suddenly increases can be identified reasonably well (points marked X). The liquid rates etc. at points X were used to calculate the vapor entrainment rates. In these calculations it was assumed that either no segregation occurs ($\epsilon_{g,s} = \bar{\epsilon}_{g,d}$) or that this segregation can be taken from the Lockett-Gharani curve. The results obtained are collected in Table 3.

It is concluded from the above table that especially at the highest pressures large amounts of vapor are entrained with the downcomer underflow. Moreover, the data for "no segregation" are perhaps more realistic than the data for "with segregation."

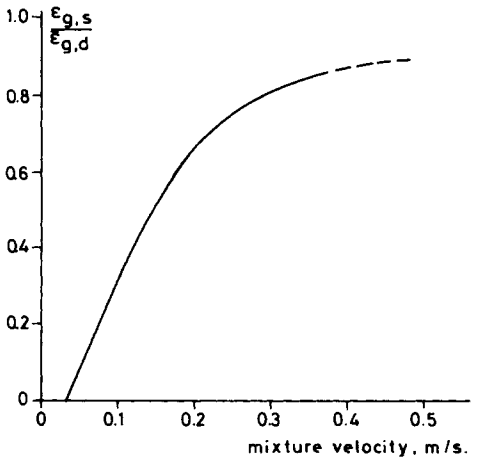

Figure 4. Ratio of vapor fraction in downcomer underflow and average vapor fraction in downcomer.

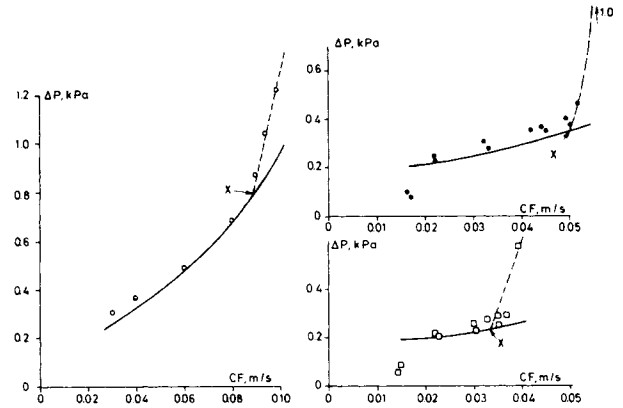

Figure 5. Pressure drop of high-pressure FRI runs: full lines, calculated by Eq. 10; "X", incipient flooding points.

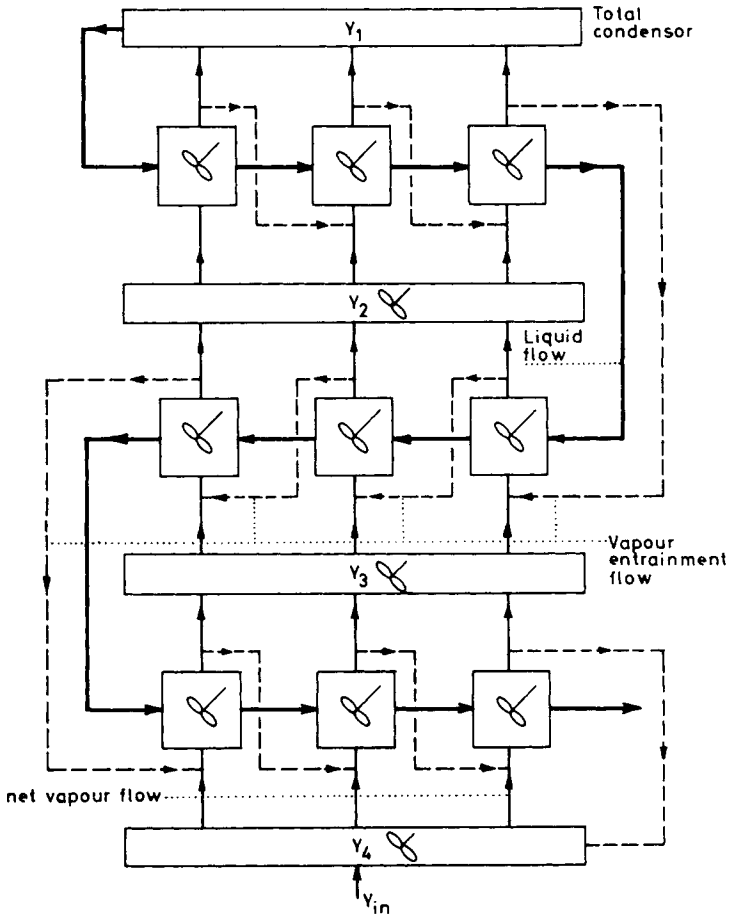

Figure 6. Vapor entrainment—efficiency model; three mixing zones per tray.

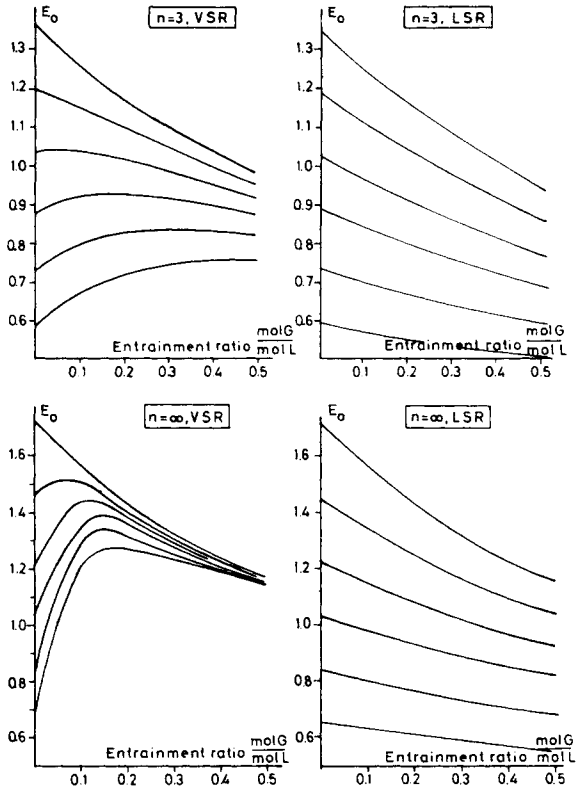

Figure 7. Effect of vapor entrainment on overall cascade efficiency.

VSR: vapor side driving force relevant

LSR: liquid side driving force relevant

VAPOR ENTRAINMENT—EFFICIENCY MODEL

For the development of the efficiency model—described in more detail in the Appendix—the tray is assumed to be divided into mixing zones. In each zone the liquid is ideally mixed and the vapor flows through the zone in plugflow. The liquid entering and leaving the zones carries the same amount of vapor per mol of liquid as the liquid entering the tray from the downcomer slot opening. The composition of the entrained vapor is taken equal to the composition of the total vapor leaving the top of a previous zone and it is assumed to be mixed completely with the vapor entering the zone from the tray below. The vapor leaving the zones is assumed to be ideally mixed before entering the next higher tray. The model is schematically illustrated in Figure 6. The calculations were made for $\lambda = 1$, (which is representative for the C_4-fractionation) and for 3 to 10 trays in the total cascade; the results were expressed in terms of overall cascade tray efficiency (E_o). Since in C_4-fractionation the flow on the trays can be taken as plugflow, the calculations were made for 1, 3, 6 and 12 mixing zones per tray in order to allow extrapolation to infinite mixing zones (= plug flow).

An important aspect of the calculations concerned the definition of the point efficiency (= mixing zone efficiency) in terms of either vapor-side Murphree efficiency ($E_{p,g}$, vapor side driving force relevant, VSR) or liquid side Murphee efficiency (liquid side driving force relevant, LSR). The application of the latter needs some explanation, which is given in the Appendix. The effect of vapor entrainment on E_o turnes out to be quite different if either the vapor side or the liquid side is taken as controlling. As a matter of fact, vapor entrainment in the case of low $E_{p,g}$ is generally beneficial for the cascade E_o. In the case that the liquid side driving

TABLE 3. ENTRAINMENT RATIOS

Pressure kPa	Liquid Rate m³/h	No Segregation $\bar{\epsilon}_{g,d} = \epsilon_{g,s}$	No Segregation kmolG/kmolL	With Segregation $\bar{\epsilon}_{g,d}$	With Segregation $\epsilon_{g,s}$	With Segregation kmolG/kmolL
1,140	64.2	0.57	0.075	0.59	0.52	0.05
2,070	53.0	0.73	0.36	0.74	0.64	0.24
2,760	43.8	0.75	0.67	0.77	0.66	0.43

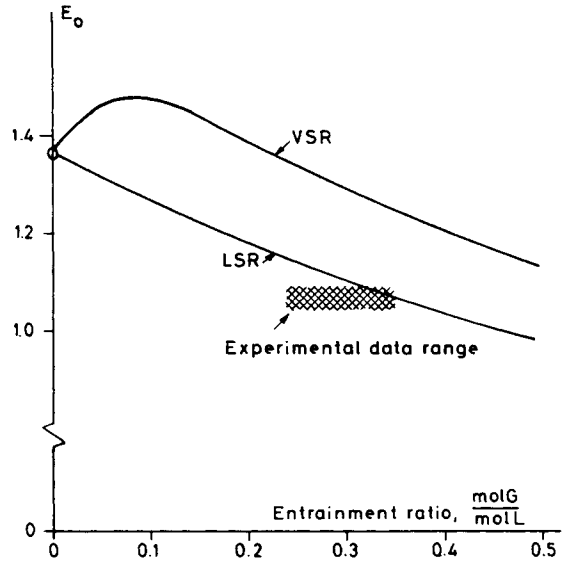

Figure 8. Comparison of predicted overall cascade efficiency with observed values (2,070 kPa, assumed E_{pog} = 87%)

VSR: vapor side driving force relevant

LSR: liquid side driving force relevant

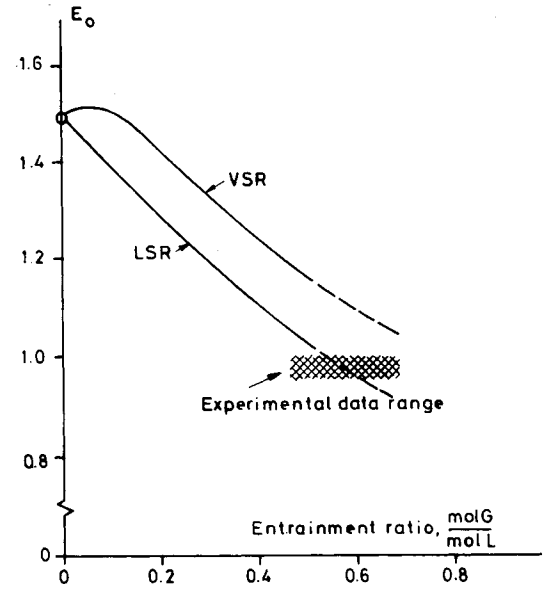

Figure 9. Comparison of predicted overall cascade efficiency with observed values (2,760 kPa, assumed $E_{p,og}$ = 91%).

VSR: vapor side driving force relevant

LSR: liquid side driving force relevant

force is taken relevant, E_o is steadily decreasing with entrainment. This is illustrated in Figure 7 in which four calculated cases (for 3–10 trays in the cascade) have been plotted.

The explanation of these surprising differences follows from the fact that with $E_{p,g}$, vapor entrainment acts as a recycle. This causes that more volatile component is stripped out of the liquid, i.e., the zone efficiency is increased. This effect is in part compensated by the overall effect of vapor backmixing over the total cascade. The latter becomes controlling at very high $E_{p,g}$'s. On the other hand, with liquid side driving force being relevant, the cascade backmixing effect is the only mechanism present. This explains the monotonous decrease of E_o with entrainment for all levels of E_o.

DISCUSSION

The two sets of curves for infinite mixing zones in Figure 7 provide the quantitative basis for the loss in E_o at high pressures. However, apart from the entrainment rates we need information on the overall efficiency without entrainment. It is proposed to derive these from the point efficiencies, taken from the plot of point efficiency against reduced pressure, in which the data with negligible or low entrainment (C_6 data, C_4 at 1,140 kPa) are extrapolated to 100% efficiency at the critical point. Two different methods of extrapolation were applied, i.e., extrapolation against P_R as shown in Figure 3 and extrapolation against flow parameter, assuming 100% efficiency at FP = 1 (since the efficiency data were taken at total reflux). The first method gives somewhat higher values then the second method. In this manner estimated entrainment free point efficiencies and overall efficiencies are:

Pressure, kPa	$E_{p,og}$, %	E_o, %
2,070	85–88	134–141
2,760	89–92	144–151

From Figure 7, curves have now been interpolated for entrainment free E_o values, identical with the average of the above E_o's. These curves are plotted in Figures 8 and 9. Also indicated are the entrainment ratios with and without segregation (Table 3) and the measured range of E_o's. We see that especially in the case that liquid-side driving force is relevant, the observed data range comes quite close to the calculated curves.

Although the above analysis is rather speculative, it is believed that in total rather solid evidence has been established on the detrimental effect of vapor entrainment on tray efficiency at very high pressures. The real mass transfer on the trays is apparently much better than would follow from the observed overall efficiencies. Therefore the observed efficiencies are as such unsuitable for development of mass transfer correlations. As an approximation for the real mass transfer rates the authors would recommend the use of the "extrapolated point efficiencies."

NOTATION

b = weir length per unit bubbling area, m^{-1}
C_d = discharge coefficient
CF = capacity factor, $u_g\ (\rho_g/\Delta\rho)^{1/2}$ m/s
D = column diameter, m
E_{mog} = Murphee plate efficiency, overall gas side
E_o = overall cascade plate efficiency
$E_{p,g}$ = point efficiency, gas side
$E_{p,og}$ = point efficiency, overall gas side
$E_{z,mg}$ = zone efficiency, gas side
$E_{z,ml}$ = zone efficiency, liquid side
F = liquid rate, mol/s
FP = flow parameter $(u_l/u_g)(\rho_l/\rho_g)^{1/2}$
G = quantity of entrained vapor, mol
g = acceleration gravity, m/s^2
ΔH = liquid back up in downcomer, m
H_T = tray spacing, m
H_W = weir height, m
h_l = liquid holdup on tray, m
L = quantity of entraining liquid, mol
LSR = liquid side driving force relevant
n = number of mixing zone's on tray
ΔP = tray pressure drop, Pa
Pe = Peclet number
P_R = reduced pressure
u_g = superficial vapor velocity on bubbling area, m/s
$u_{g,h}$ = vapor velocity in holes of sieve tray, m/s
u_l = superficial liquid velocity on bubbling area, m/s
$u_{l,s}$ = liquid downcomer slot velocity, m/s

u_m = vapor-liquid mixture downcomer slot velocity, m/s
V = total vapor rate per mixing zone, mol/s
VSR = vapor-side driving force relevant
w = weir length, m
X = liquid composition
Y = vapor composition
β^2 = square root of the ratio of downcomer underflow area to downcomer crossectional area
$\epsilon_{g,d}$ = average vapor fraction in vapor-liquid mixture in downcomer
$\epsilon_{g,s}$ = vapor fraction in vapor-liquid mixture flowing through downcomer slot
λ = stripping factor
$\Delta\rho$ = difference in density between liquid and vapor, kg/m^3
ρ_g = vapor density, kg/m^3
ρ_l = liquid density, kg/m^3
ρ_m = average density of vapor-liquid mixing flowing through downcomer slot, kg/m^3

LITERATURE CITED

Barker, P. E., and M. F. Self, "The Evaluation of Liquid Mixing Effects on a Sieve Plate Using Unsteady and Steady State Tracer Techniques," *Chem. Eng. Sci.*, **17**, 541 (1962).

Gester, J. A., "Bubble Tray Design Manual," AIChE, p. 47 (1958).

Hofhuis, P. A. M., "Flow Regimes on Sieve Trays for Gas/Liquid Contacting," Thesis, Technical University Delft (June 4, 1980).

Lockett, M. J. and A. A. W. Gharani, "Downcomer Hydraulics at High Liquid Flow Rates," *I. Chem. E. Symp. Ser.*, No. 56, p. 2.3/43.

Porter, K. E. and J. D. Jenkins, "The Interrelationship between Industrial Practice and Academic Research in Distillation and Absorption," *I. Chem. E. Symp. Ser.*, No. 56, Supplementary Discussion Volume, p. 75 (1979).

Porter, K. E., M. J. Lockett, and C. T. Lim, "The Effect of Liquid Channeling on Distillation Plate Efficiency," *Trans. I. Chem. E.*, **50**, 91 (1972).

Porter, K. E., A. Safekourdi, and M. J. Lockett, "Plate Efficiency in the Spray Regime," *Trans. I. Chem. E.*, **55**, 190 (1977).

Sakata, M. and T. Yanagi, "Performance of a Commercial Sieve Tray," *I. Chem. E. Symp. Ser.*, No. 56, p. 3.2/21 (1979).

Manuscript received March 4, 1981; revision received August 5, and accepted August 24, 1981.

APPENDIX

Vapor Entrainment Calculations

The basis of the vapor entrainment model are the calculations around a mixing zone (Figure A1). For these calculations the mass-balance around the mixing zone, the equilibrium relationship and a description of the mass-transfer efficiency in the mixing zone are needed.

Mass balance:

$$F(X_{z,\text{in}} - X_{z,\text{out}}) = V(Y_{z,\text{out}} - Y_{z,\text{in}})$$

For the equilibrium between vapor and liquid it is assumed that

$$Y^*_{z,\text{out}} = X_{z,\text{out}} + \text{constant}$$

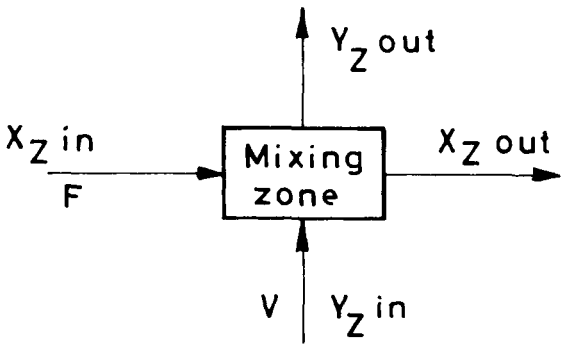

Figure A1. Mixing zone.

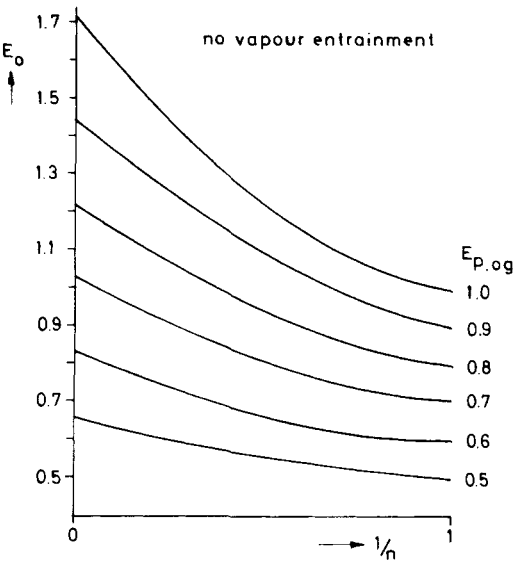

Figure A2. E_o as function of mixing zone efficiency (no entrainment).

which approximately holds for the case of high pressure butanes distillation under consideration.

The mass-transfer efficiency is described as a Murphee efficiency. The Murphee efficiency of the mixing zone can be based either on the vapor-phase or on the liquid-phase concentration change, i.e.

$$E_{z,mg} = \frac{Y_{z,\text{out}} - Y_{z,\text{in}}}{Y^*_{z,\text{out}} - Y_{z,\text{in}}}$$

Murphee zone efficiency based on the vapor phase driving force (VSR)

$$E_{z,ml} = \frac{X_{z,\text{in}} - X_{z,\text{out}}}{X_{z,\text{in}} - X^*_{z,\text{out}}}$$

Murphree zone efficiency based on the liquid phase driving force (LSR)

$E_{z,mg}$

In the case of a vapor-phase based Murphree mixing zone efficiency $E_{z,mg}$ is equal to the point efficiency $E_{p,og}$. The effect of vapor entrainment has been calculated for values of $E_{z,mg}$ ranging from 0.5 to 1.0 and with 1, 3 and 12 mixing zones per tray. In this way the calculations can be extrapolated to plug-flow, i.e., at $n = \infty$ or $1/n = 0$ (Figure A2).

As can be seen from Figure A2 and Table A1, when no vapor entrainment is present, the values of the overall column efficiency (E_o) extrapolate to the expected values for plug-flow (Table A1). The effect of vapor entrainment on column efficiency for three mixing zones per tray and for plug-flow is given in Figure 7.

$E_{z,ml}$

The values of $E_{z,ml}$ are not the same as the point efficiencies,

TABLE A1. OVERALL COLUMN EFFICIENCY AS A FUNCTION OF THE POINT-EFFICIENCY, $E_{p,og} = E_{z,mg}$

$E_{z,mg}$ (= $E_{p,og}$)	E_o, Ideal Mixing	E_o, Plug-Flow
1.0	1.0	1.72
0.9	0.9	1.46
0.8	0.8	1.23
0.7	0.7	1.01
0.6	0.6	0.82
0.5	0.5	0.65

TABLE A2. DETERMINED VALUES OF $E_{z,ml}$ USED IN THE CALCULATION OF E_o

1-Zone/Tray $E_{z,ml}$ (= $E_{z,mg}$)	3-Zones/Tray $E_{z,ml}$	12-Zones/Tray $E_{z,ml}$
0.5	0.250	0.0775
0.6	0.333	0.1139
0.7	0.445	0.1707
0.8	0.570	0.254
0.9	0.760	0.437
1.0	1.0	1.0

since for the liquid flow the mixing zones are arranged in series. For this reason the value of the mixing zone efficiency has to be determined in such a way that for no vapor entrainment the overall column efficiency E_o for every case corresponds with the E_o's calculated on the basis of $E_{z,mv}$. In this way Figure A2 also applies for the calculations based on $E_{z,ml}$. The values of $E_{z,ml}$ are given in Table A2.

The values of $E_{z,ml}$ given in Table A2 are used to calculate the effect of vapor entrainment on the overall column efficiency. The results for three mixing zones per tray and for plug-flow are given in Figure 7.

Intraparticle-Forced Convection Effect in Catalyst Diffusivity Measurements and Reactor Design

Intraparticle forced convection was considered in order to explain experimentally observed changes in effective diffusivity (apparent) with flowrate, when measures are carried out in fixed beds.

A complete model taking into account intraparticle diffusion and forced convection together with film diffusion is derived in order to analyze diffusivity measurements by physical methods, both in perfectly mixed reactors and fixed beds.

The experiments were carried out with hydrogen tracer in a partial oxydation catalyst.

Implications of the use of such "apparent" effective diffusivities in reactor design are discussed, showing that errors of 100% can be made.

A. E. RODRIGUES

Department of Chemical Engineering
University of Porto
Porto Codex, Portugal

BUM J. AHN
and
ANDRÉ ZOULALIAN

Département de Génie Chimique
Université de Technologie de Compiègne
Compiègne, France

SCOPE

Experimental data on effective diffusivities, measured by unsteady state techniques show that increasing the flowrate, greater values for the effective diffusivity (apparent) are obtained (Boersma-Klein and Moulijn,, 1979; Ahn, 1980). These findings have been sometimes explained by measurements inaccuracies, but this explanation can hardly be acceptable when changes on apparent effective diffusivities are of one order of magnitude for the same changes in flowrate.

On the other hand Nir and Pismen (1977) analyzed the influence of intraparticle-forced convection on effectiveness factors, showing that this mechanism can be important for large pore catalysts, specially with liquid phase reactions.

In the present work, we tried to explain the results obtained in a series of experiments carried out over a range of flowrates corresponding to changes of one order of magnitude in Reynolds number (Re = 10 to 100) for hydrogen, as a tracer, in a highly porous catalyst for the partial oxydation of butene to maleic anhydride (Rhone Poulenc BM 329). The questions to be answered are: Can intraparticle forced convection explain the variation of the measured effective diffusivity with flowrate? If so, how do we predict the intraparticle convection velocity for given operating conditions?

Finally the aim of this work was to check if, for practical purposes, significant implications result when apparent effective diffusivities are used in reactor design.

CONCLUSIONS AND SIGNIFICANCE

A series of experiments for the measurement of effective diffusivity was carried out in a fixed bed of small tube diameter/particle diameter ratio—single pellet string reactor of Scott et al. (1974)—using hydrogen as nonadsorbable tracer and a Rhone Poulenc BM 329 catalyst (catalyst used for partial oxydation of butene to maleic anhydride based on vanadium and phosphorus oxydes) at 293 K.

Sharp variations of the measured effective diffusivity with flowrate were observed, the values being obtained from optimization based on a transfer function of the system which takes into account only one mechanism inside the particle (intraparticle diffusion).

We investigated if intraparticle-forced convection could explain these findings. We first developed the model equations and the transfer functions of the current systems for physical measurements of effective diffusivity.

We were able to show that the measured (apparent) effective diffusivity, $\tilde{D}_{eff}$, is related to the true (constant) effective dif-

Correspondence concerning this paper should be addressed to A. E. Rodrigues.
0001-1541-82-5941-0541-$2.00.